EFFECT OF CERAMIC NANOCOMPOSITE SUPPORTS ON CATALYTIC ACTIVITY OF PLATINUM CATALYSTS FOR FUEL CELLS

Rabia Naeem, Riaz Ahmed**† & Muhammad Shahid Ansari**

ABSTRACT

Ceramics Al_2O_3 and TiO_2 were mixed with carbon as hybrid supports for platinum catalyst and their catalytic activities were studied in basic media. X-ray diffraction studies showed the formation of platinum nanoparticles of 7 to 9 nm sizes on the composites and other supports. Energy dispersive X-ray spectroscopy (EDX) showed the composition of catalysts. Cyclic voltammetry was used for the determination of peak current, specific activity, mass activity and stability of the catalysts for the electro oxidation of methanol in basic media. Composite supported catalysts, including Pt/TiO_2-C and Pt/Al_2O_3-C, showed much higher catalytic activities and stability as compared to Pt-C, Pt-Al_2O_3 and Pt-TiO_2 catalysts. Exchange current densities were measured from Tafel plots; heterogeneous rate constants were also measured and were found to be substantially higher for composite supported catalysts. Titania-Carbon supported catalyst has higher catalytic activity as compared to Alumina-Carbon supported catalysts. Ceramic-Carbon supported platinum catalysts showed much higher catalytic activity and stability and can be helpful for the commercialization of low temperature fuel cells.

Keywords: *Ceramics, Carbon, Nano composites, Platinum catalysts, Characterization*

1. INTRODUCTION

Demand for energy is increasing that is mostly met by burning of fossil fuels, including coal, petroleum and natural gas, which causes enormous pollution (Duic, et al., 2013; Panwa, et al., 2011). Use of fossil fuels is not sustainable for future applications because of pollution and climate change effects (DOE, 2013). A lot of work is being done for the development of renewable energy sources (solar, wind, hydro & biomass, etc) and alternative energy sources (hydrogen, fuel cells, batteries, etc;) for sustainable energy (Duic, et al., 2013).

Fuel cells are emerging as clean and efficient alternative energy sources (Costamagana & Srinivasan, 2001; Ren, et al., 2000; Chalk & Miller, 2006). Fuel cell technology offers an attractive combination of highly efficient fuel utilization and environment-friendly operations (Mueller, et al., 2015; Romero-Pascual & Soler, 2014; Wang & Nehrir, 2008).

Polymer electrolyte membrane (PEM) fuel cells are potential energy sources for transportation and many other stationary and portable uses (Casolari, et al., 2014). Stability and efficiency are the major concerns for their commercialization. During operation, degradation of carbon support takes place due to corrosion, which leads to their low performance (Borup, et al., 2006; Speder, et al., 2014). Therefore, there is a need to decrease the overall cost and increase the efficiency and durability for widespread commercial use of fuel cells. Ceramic-carbon composites have shown a good potential to overcome this problem (Antolini & Gonzalez, 2009; Shao, et al., 2009; Armstrong, 2012).

In this study composite supports, including titania, alumina and carbon were used to prepare composite supports for platinum catalysts. Platinum catalysts that supported only on carbon or ceramics were also prepared, and their catalytic activities and durability were studied and compared.

2. MATERIALS AND METHODS

2.1 Synthesis of Catalysts

Vulcan carbon XC-72 was used having surface area of 254 $m^2 g^{-1}$ and average particle size of 30 nanometer. It was purified by refluxing it at 60°C with concentrated HCl and ultra-sonification. Treated Vulcan carbon was filtered, washed and dried it at 110°C. It was functionalized by treating it with 4:1 v/v mixture of 8M HNO_3 and H_2O_2. Analytical grade titania and alumina were used as received.

Pt/Vulcan carbon (10 wt. % Pt) catalyst was synthesized using conventional reduction method under argon atmosphere at room temperature, and using $NaBH_4$ as reducing agent. Aqueous solution of $PtCl_4$ with Vulcan carbon was stirred and $NaBH_4$ solution was added in the solvent mixture drop by drop. Black suspension was filtered and washed several times with de-ionized water till neutral pH of the filtrate was vacuum-dried for 24 hrs at 110°C.

For the synthesis of Pt/TiO_2-C and Pt/Al_2O_3-C, nanocomposite TiO_2 and Vulcan carbon were added into water: 2-propanol (3:1 v/v) mixture (the solvent) and ultra sonicated for 1 hour. The black solid was filtered, washed and dried in vaccum oven for 24 hours at 110°C. Then Pt (10 wt. %) was loaded on this

* Department of Chemistry, Quaid-i-Azam University, Islamabad, Pakistan

*&** COMSATS Headquarters, Shahrah-e-Jamhuriat, G-5/2, Islamabad, Pakistan. †E-mail: riaz_ecfc@yahoo.com

mixed/composite support by conventional co-reduction method in which $NaBH_4$ was used as a reducing agent. The resulting black suspension of Pt/TiO_2-C and Pt/Al_2O_3-C nanocomposite catalysts was filtered, washed and vacuum-dried for 24 hours at 110°C. For the preparation of Pt/TiO_2 and Pt/Al_2O_3 catalysts, the procedure was the same however no carbon was added.

2.2 Characterization of Catalysts

X-ray diffraction studies were made at room temperature by using X-ray Diffractrometer (3040/60 X'pert PRO) using Ni-filtered Cu-Ka radiations (40 kV, 30 mA). Energy dispersive X-rays spectra (EDX) were recorded by using JEOL LA-6490, in energy ranged from 0 – 20 keV using ZAF method of qualitative analysis. Eco Chemie Autolab PGSTAT 12 potentiostat/galvanostat, Netherlands, with the electrochemical software package GPES 4.9 was employed for cyclic voltammetric measurements, using a three-electrode system for electrochemical studies under argon atmosphere at ambient temperature. Graphite electrode was used as working electrode with exposed polished tip of 0.785 cm^2 surface area. About 20 mg catalyst was ultrasonically dispersed in 1 mL of aqueous 2-propanol in a test tube for 30 minutes and 60 μL of the resulting suspension was spread on the tip. The solvent was evaporated, 10 μL Nafion solution (5%) was applied to the tip and finally dried in air. Nafion was used as an ion-exchange binder. Cyclic voltammograms were measured in the potential range from -1.0 to +0.5 V vs. SCE in the aqueous medium containing 0.2 M CH_3OH (Sigma Aldrich, 99.7%) and 0.5 M KOH (Fluka, 99%).

3. RESULTS AND DISCUSSIONS

3.1 X-ray Diffraction Analysis

Figures 1 and 2 show the XRD patterns of Pt/TiO_2-C, Pt/TiO_2, Pt/C and Pt/Al_2O_3-C, Pt/Al_2O_3, Pt/C. For Pt/TiO_2, peaks situated at 25.3° and 48° are due to anatase (101) and (200) lattice planes, respectively. The peak at 55.5° may result from the overlap of the two adjacent peaks due to the anatase (211) and (105) lattice planes. The three diffraction peaks were weak and broad indicating poor crystallinity (Chen & Pan, 2009). Whereas, in Pt/TiO_2-C nanocomposite TiO_2 anatase peak appeared at 25.5° of (101) plane, which overlaps the carbon peak of (002) lattice plane at 26° in Figure-1.

Crystallographic parameters, such as lattice constants (a and c), unit cell volume (V_{cell}), crystallite size (D) and X-ray density (d_x) were calculated from the obtained data. Crystallite size of all the samples was calculated by using Debye-Scherrer equation (Rajalakshmi, et al., 2008; Ahmed, et al., 2009).

$$D = \frac{k\lambda}{\beta \cos\theta} \quad (1)$$

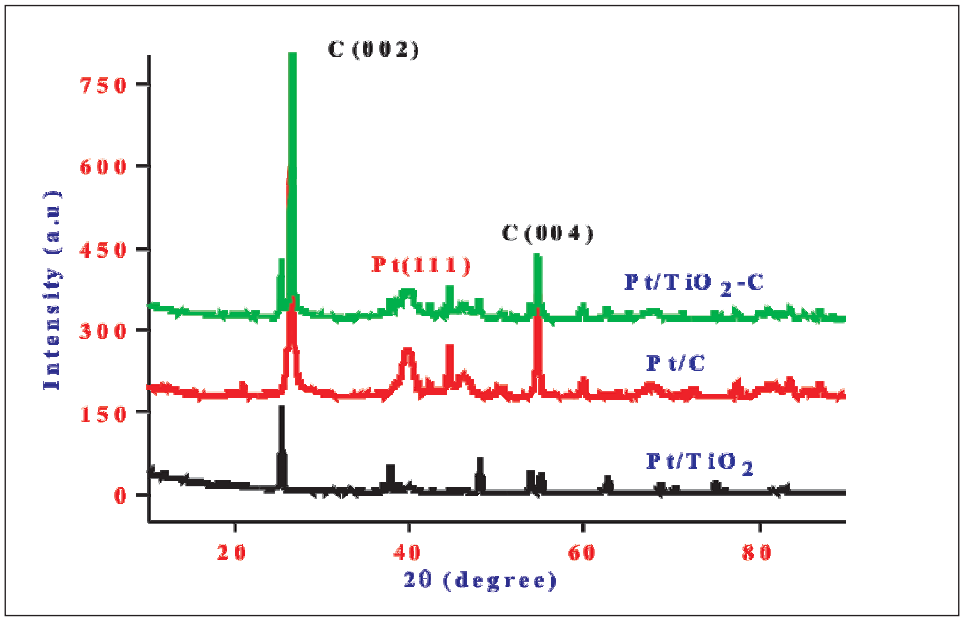

Figure-1: XRD Patterns of Pt/TiO_2-C, Pt/TiO_2 and Pt/C

Table-1: XRD Parameters Evaluated for Pt/TiO_2-C, Pt/TiO_2 and Pt/C

Catalyst	Position 2θ (degree)	d-spacing A	Lattice parameter a/A	Cell volume V/A^3	Density $\rho_{X\text{-}ray}$ g cm^{-3}	Ave. crystallite size (D/nm)
Pt/TiO_2-C	39.8	2.265	3.9229	60370	20.86	7.16
Pt/TiO_2	39.93	2.258	3.9105	59.8	21.06	8.9
Pt/C	39.66	2.25	3.8987	59.26	21.06	7.96
Pt Standard Pattern	39.67	2.27	3.912	59.87	21.52	-

Where k is the constant and its value is 0.89 (Cullity, 1956; Shao, et.al., 2010), λ is 1.54 A, θ is the angle and β is the full width at the half maximum or the broadening of the diffraction line measured at half its maximum intensity. The lattice constants are obtained by solving the simultaneous equations obtained by putting different d and h,k, and l values in equation.

$$\frac{1}{d^2} = \frac{h^2 + k^2}{a^2} + \frac{l^2}{c^2} \qquad (2)$$

In this equation 'd' is the d-spacing, 'h', 'k' and 'l' are the corresponding indices of each line in the pattern. The lattice constant 'a', volume of cell 'V_{cell}' and X-ray density '$\rho_{x\text{-}ray}$' (g cm^{-3}), is obtained by the following equations (Rajalakshmi, et al., 2008; Cullity, 1956).

$$a = \left[d^2(h^2 + k^2 + l^2)\right]^{1/2} \qquad (3)$$

$$V_{cell} = a^3 \qquad (4)$$

$$\rho_{x-ray} = \frac{ZM}{V_{cell} N_A} \qquad (5)$$

where 'M' is the molar mass of the sample, 'N_A' the Avogadro's number, 'Z' is the number of molecules per unit cell (Z=4 for Pt cubic-type) and 'V_{cell}' is the unit cell volume.

The particle size of platinum in hybrid support is smaller than Pt/C and Pt/TiO_2 (Table-1). While for Pt/Al_2O_3, all the four broad peaks of platinum at 39°, 46°, 68°, and 81° are prominent because Al_2O_3 is s° amorphous that not a single sharp peak of this oxide appeared (Figure-2). In case of Pt/Al_2O_3-C, the broadening of the diffraction peak for platinum indicates a reduction in the average crystallite size from Pt/C. That is why Pt crystallite size in Pt/Al_2O_3 is

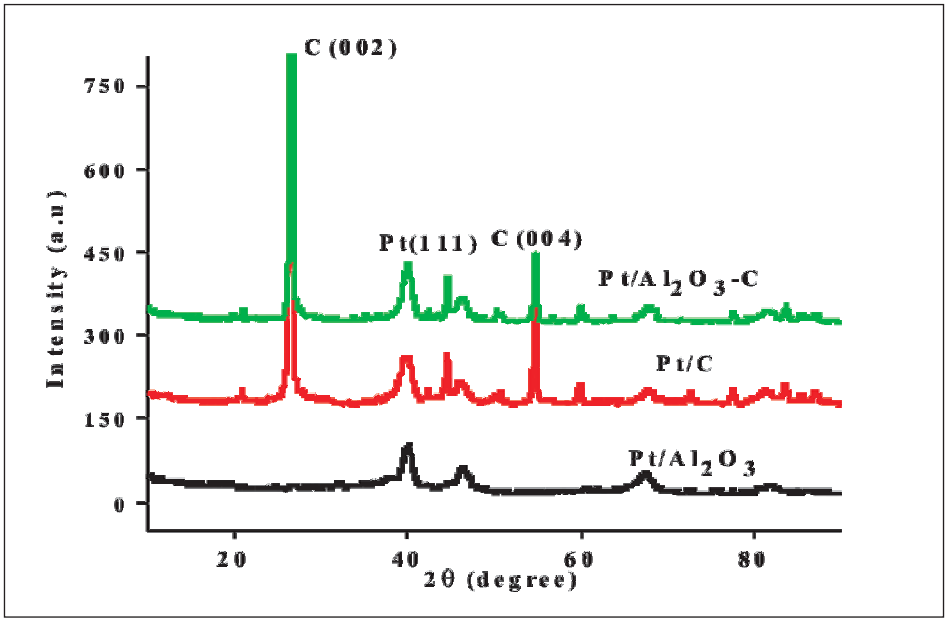

Figure-2: XRD Pattern of Pt/Al_2O_3-C, Pt/Al_2O_3 and Pt/C

Table-2: XRD Parameters Evaluated for Pt/Al_2O_3-C, Pt/Al_2O_3 and Pt/C

Catalyst	Position 2θ(degree)	d-spacing A	Lattice parameter a/A	Cell volume V/A^3	Density $\rho_{X\text{-}ray}$ g cm^{-3}	Ave. crystallite size (D/nm)
Pt/Al_2O_3-C	40.02	2.253	3.9024	59.43	21.2	8.95
Pt/Al_2O_3	40.12	2.251	3.8992	59.28	21.25	6.7
Pt/C	39.66	2.25	3.8987	59.26	21.06	7.96
Pt Standard Pattern	39.67	2.27	3.912	59.87	21.52	-

Table-3: Compositional Analysis of Catalysts from EDX Results

Catalysts	C %	Pt %	Ti%	Al%	O %	Total
Pt/TiO_2-C	77.4	9.76	5.2	-	7.6	100
Pt/TiO_2	-	9.58	59	-	40	100
Pt/Al_2O_3-C	77.7	8.92	-	4.8	8.5	100
Pt/Al_2O_3	-	9.07	-	53	47	100
Pt/C	86	9.16	-	-	4.64	100

Table-4: Activity Parameters Evaluated from CVs in 1M CH_3OH + 1M KOH on Various Catalysts

Catalysts	Peak potential E_p/V	Peak Current I_p/(mA)	Specific activity j/mA.cm^{-2}	Mass activity mA/mg Pt
Pt/C	-0.153	26.37	33.592	165
Pt/TiO_2	-0.286	2.78	3.5414	23
Pt/TiO_2-C	-0.148	38.65	49.235	241
Pt/Al_2O_3	-0.265	4.52	5.796	19
Pt/Al_2O_3-C	-0.109	36.45	46.433	228

smaller than Pt/C and Pt/Al_2O_3-C (Table-2). In case of Pt/Al_2O_3 nanocomposite peak of aluminum oxide has not appeared but its presence can cause a shift in peak and also decrease the particle size of Pt in Al_2O_3-C support.

3.2 Energy Dispersive X-ray Analysis

EDX was used to ascertain the composition of catalysts for the rapid EDX analysis of chemical composition of each catalyst. LA-6490 analyzer was connected to a scanning electron microscope (SEM, LA-6490), with the incident electron-beam energies ranged from 0 to 20 keV, which impinges the sample surface from the normal angle. The measurement time was 55-58 s, and the EDX spectra were obtained by using Ziebold and Ogilvie α-Factor (ZAF) correction for the quantitative analysis of metal alloys (Shao, et.al., 2010).

Table-3 shows the EDX results of Pt/TiO_2-C, Pt/TiO_2, Pt/Al_2O_3-C, and Pt/Al_2O_3 catalysts corresponding to the compositions of metals. Large amount of oxygen is observed in case of ceramic support and mixed support as compared to carbon. Composition of catalysts as determined from EDX are given in Table-3. It can be seen that the amounts of different constituents in the catalysts are nearly the same as added earlier, except for some additional oxygen which is attached to carbon due to its functionalization.

3.3 Electrocatalytic Activity of Catalysts in Basic Medium

Electrocatalytic activity of various synthesized catalysts for methanol oxidation was determined in basic medium using KOH solution by cyclic voltammetry. The parameters determined are: peak current (I_p), specific activity (I_s), mass activity (I_m) and exchange current density (i_o). Figures 3 and 4 show CVs measured in CH_3OH + KOH solutions at scan rate 50 $mV.s^{-1}$ from -1.0 to 0.5V on the catalysts. In anodic sweep, a well-defined and sharp forward anodic peak was observed near -0.2V, while in cathodic sweep very

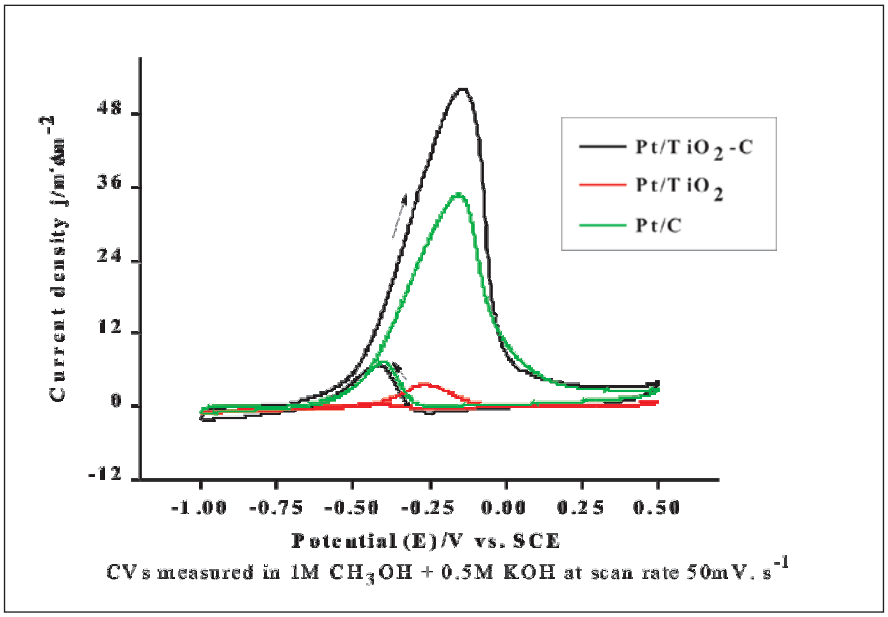

Figure-3: CVs Measured in 1M CH_3OH + 1M KOH at 50 $mV.s^{-1}$ on Pt/TiO_2-C, Pt/TiO_2 and Pt/C

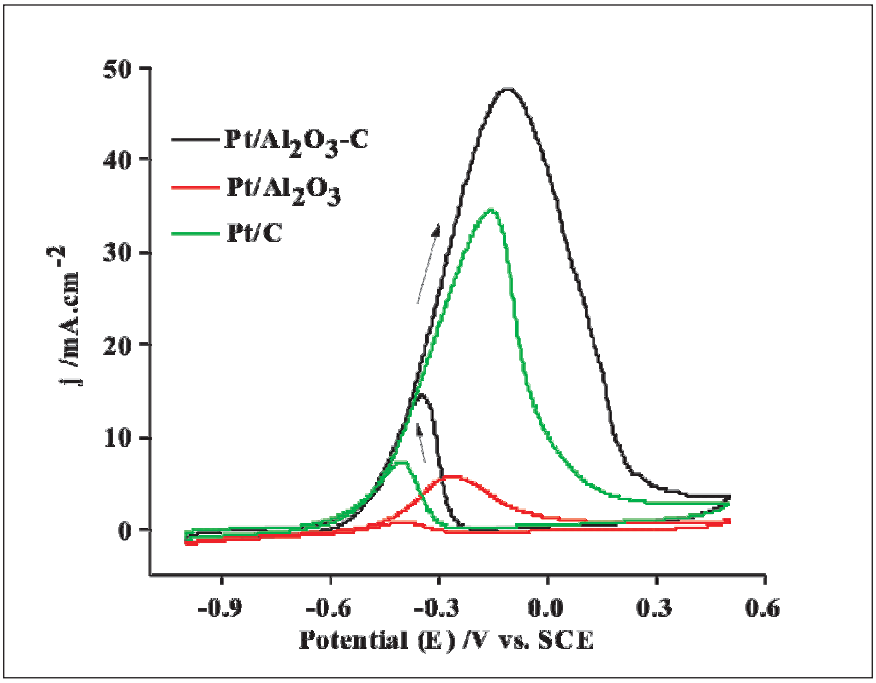

Figure-4: CVs Measured in 1M CH_3OH + 1M KOH at 50 $mV.s^{-1}$ on Pt/Al_2O_3-C, Pt/Al_2O_3 and Pt/C

small reverse anodic peak was observed of the methanol oxidation. Here, in Table-4 highest values of I_p, I_s and I_m were observed for Pt/TiO_2-C and Pt/Al_2O_3-C than Pt/C, Pt/TiO_2 and Pt/Al_2O_3. The comparison of all synthesized catalysts (Table-4) corroborated that in basic medium Pt/TiO_2-C and Pt/Al_2O_3-C showed higher catalytic activity. While in the case of Pt/TiO_2 and Pt/Al_2O_3 very low values of current were observed. Higher electrocatalytic activity for the methanol oxidation for Pt nanoparticles loaded on mixed support than ceramic support, which again shows that Pt has a larger utilization in hybrid ceramic supported nanocatalyst. The methanol oxidation in terms of mass activity of the Pt/TiO_2-C was much higher than that of

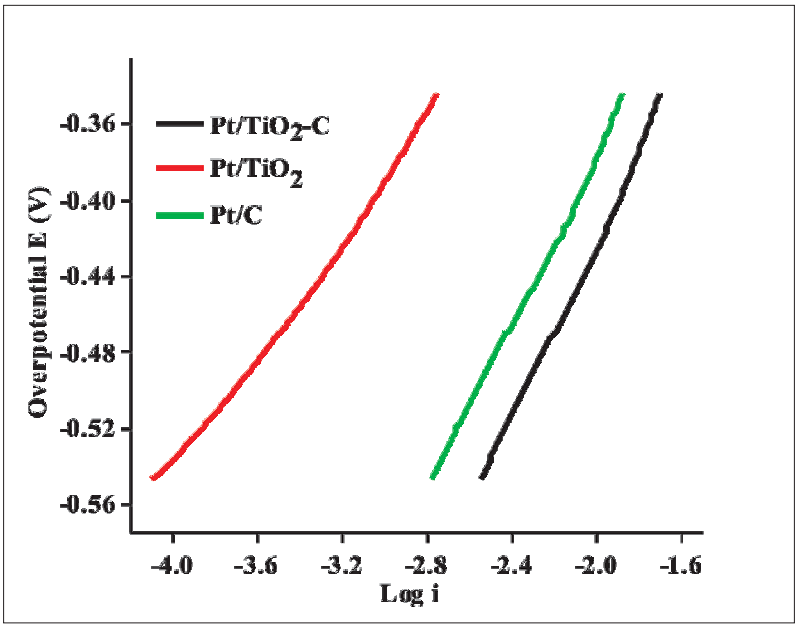

Figure-5: Anodic Polarization Curves Measured in 1M CH_3OH + 1M KOH at 50 $mV.s^{-1}$ on Pt/TiO_2-C, Pt/TiO_2 and Pt/C

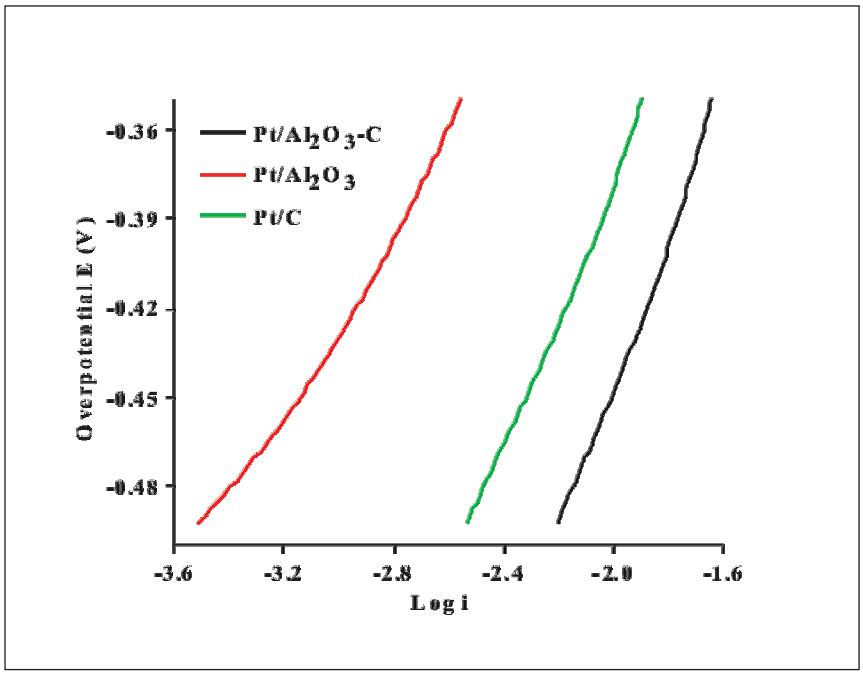

Figure-6: Anodic Polarization Curves Measured in 1M CH_3OH + 1M KOH at 50 $mV.s^{-1}$ on Pt/Al_2O_3-C, Pt/Al_2O_3 and Pt/C

the Pt/ TiO_2 and about 46% higher than that of Pt/C. Similarly Pt/Al_2O_3-C showed much more activity than Pt/Al_2O_3 and about 38% higher than Pt/C catalysts. Titania-based composite catalyst is slightly better than the alumina based catalyst.

3.4 Comparison of Exchange Current Densities from the Tafel Plots

Figures 5 and 6 show Tafel plots measured in basic media at scan rate of 50 mVs^{-1} on various catalysts for the oxidation of methanol. Tafel equation is written as

Table-5: Polarization Data Evaluated from Tafel Plots in 1M CH_3OH + 1M KOH

Catalysts	Tafel s slope b / (V decade $^{-1}$)	αn_α	Intercept of E vs Log i	i_omA.cm^{-2}
Pt/C	0.2107	0.281	0.0402	41.5
Pt/TiO_2	0.2163	0.273	0.0541	24
Pt/TiO_2-C	0.2314	0.256	0.0406	62
Pt/Al_2O_3	0.1529	0.387	0.0343	5.86
Pt/Al_2O_3-C	0.2522	0.235	0.0583	61.31

Table-6: Rate Constants of 1M CH_3OH in Basic Medium

Catalysts	Peak Current I_p/(mA)	Rate Constant k_{het}/cm.s^{-1} *10^{-5}
Pt/C	26.37	15.7
Pt/TiO_2	2.78	2.1
Pt/TiO_2-C	38.65	20.7
Pt/Al_2O_3	4.52	1.3
Pt/Al_2O_3-C	36.45	20

(Bard & Faulkner, 2001):

$$\Delta V_{act} = a + b \log i \quad (6)$$

Where

$$a = -2.3 (RT/\alpha F) \log i_0, \text{ and } b = 2.3 RT/\alpha F \quad (7)$$

If voltage vs log i is plotted, the main parameters, a, b, and i_o can be evaluated from the intercept and slope. The catalytic activities of catalysts can be evaluated by comparing the data of exchange current density. The values of i_o obtained from intercept are listed in Table-5. Exchange current is a measure of catalytic activity. The higher values of exchange current show higher values of catalytic activity. It is obvious from the polarization data in Table-5 that i_o increases due to presence of ceramic (metal oxides). Ceramic composite supported catalysts have much higher exchange current density than the normal carbon supported commercial catalysts. Exchange current density of only ceramic supported catalysts is also low.

3.5 Rate Constant of Methanol Oxidation

It is basically the rates of reaction which increase the efficiency of fuel cells. Higher rates of reaction show better efficiency of fuel cells. Figures 3 and 4 show the CVs measured on the nanocomposite catalysts and the irreversibility plots of methanol oxidation on nanocomposite catalysts. The peak potential (Ep^a) of forward scan increased with the increase of scan rate and a linear relationship can be obtained by plotting E_p vs. ln(ν), which indicates that the electro-oxidation of methanol is an irreversible electrode process in basic medium. Similar results were obtained for both the catalysts.

The values of heterogeneous rate constants (k_{het}) for the methanol oxidation on ceramic supported nanocomposite catalysts have been determined in basic medium using the Nicholson-Shain equation: (Ali, et.al., 2015).

$$i_p = 0.227 nFAC_o k_s.\exp[(\alpha n_\alpha.F/RT)(E_p-E_o)] \quad (8)$$

Where 'A/cm^2' is the area of the electrode, 'i_p' is the peak current, 'n' is the number of electrons transferred, 'C_o/mol.cm^{-3}' is the bulk concentration of the reactant and 'k_S/cm.s^{-1}' is the standard heterogeneous rate constant. 'F' and 'R' are the Faraday and gas constants. Reinmuth showed that for an irreversible reaction, the current flowing at the root of the wave is independent of the rate of voltage scan (Ahmed, et al., 2014). Thus the above equation can be written as:

$$i_p = 0.227 nFAC_o k_s.\exp[(\alpha n_\alpha.F/RT)(E_p-E_i)] \quad (9)$$

where 'E_i' is the potential at the root of the wave. A plot of $\ln(i_P)$ vs (E_p-E_i) at different scan rates will give rate constant from the intercept and αn_α from the slope (Table-6). As αn_α decreases the voltammogram will be more drawn out. The rate constant for Pt/TiO_2-C catalyst is much higher than it is for the others. The rate constant k_{het}/cm.s^{-1} value of 20.7x10^{-5} at 298 K for Pt/TiO_2-C is much higher than those obtained for Pt/TiO_2 and Pt/C in basic medium. Similarly, Pt/Al_2O_3-C

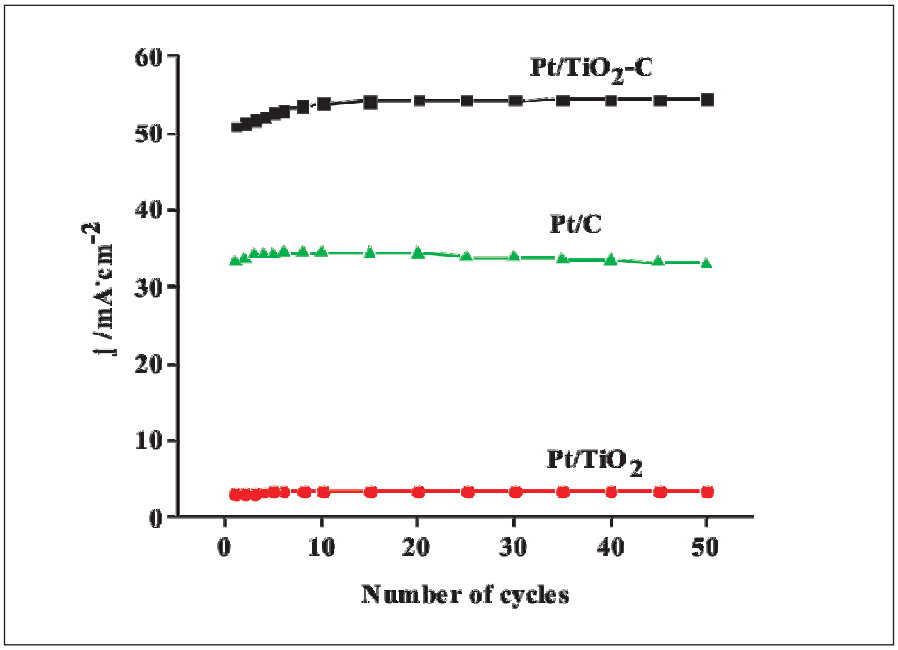

Figure-7: Durability of Pt/TiO_2-C, Pt/TiO_2 and Pt/C Catalysts in Basic Medium

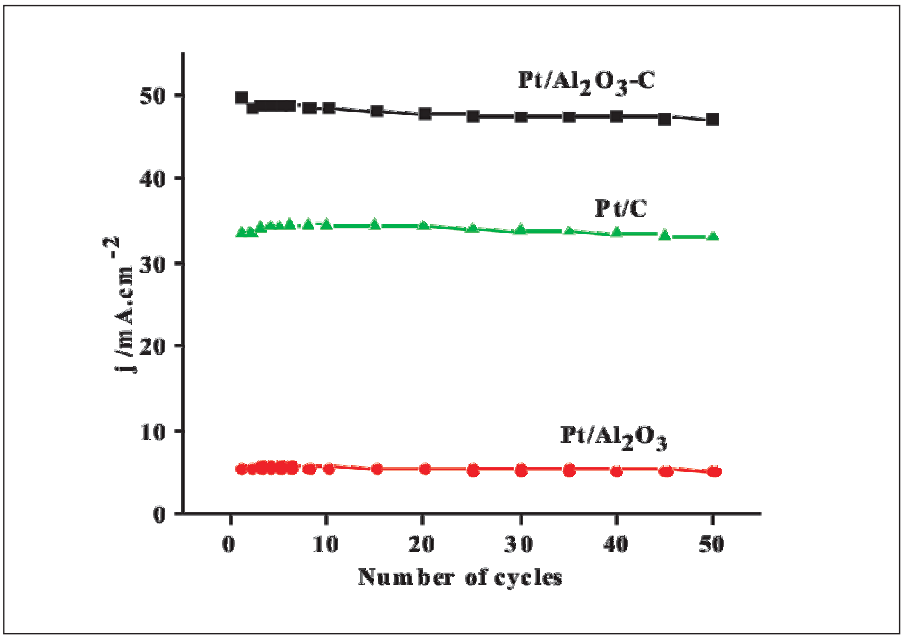

Figure-8: Durability of Pt/Al_2O_3-C, Pt/Al_2O_3 and Pt/C Catalysts in Basic Medium

has also much higher rate constant than Pt/C catalysts which are normal commercial catalysts. Here, in rate constants, it is also shown that composite catalysts are much better than the commercial catalysts.

3.6 Durability of Catalysts in Basic Medium

Figures 7 and 8 show durability of the catalysts in terms of specific activity (I_s) obtained for 1M CH_3OH + 1M KOH at scan rate 50 $mV.s^{-1}$ for fifty numbers of cycles in a single run. After each cycle, the value of specific activity increased in basic medium because

the catalyst becomes more and more active and less poisoning occurs in basic medium. Catalytic activity of Pt/TiO_2-C continued increasing with use of the catalyst. Initially, it increased rapidly and then gradually. However, in case of Pt/C catalyst the catalytic activity slightly increased only up to four cycles, then decreased up to fifty cycles due to catalyst poisoning. Catalytic activity of Pt/TiO_2 was very low as compared to other catalysts. Nearly similar is the case for alumina catalysts.

Therefore, it is concluded that Pt-NPs loaded on ceramic hybrid support are more durable than Pt on carbon. Some more durability in the case of Pt/Ceramic-carbon nanocomposite may be due to greater concentration of hydroxyl groups adsorbed on the surface of ceramic, which can easily donate active oxygen to CO-poisoned catalyst. This is how ceramics in support give not only an enhanced activity but also the better durability of catalysts. It is implied that Pt/TiO_2-C and Pt/Al_2O_3-catalysts are very promising for portable applications in direct methanol fuel cells and proton-exchange membrane fuel cells in alkaline media.

4. CONCLUSIONS

Catalysts are the most costly and important constituents for the development of fuel cells. Normally available commercial catalysts supported on carbon suffer from carbon corrosion, and consequently cause degradation of fuel cells. Efficient and durable catalysts are necessary for better operation of fuel cells. Ceramic promoted nanocomposite catalysts were synthesized and characterized. Titania-carbon composite supported platinum catalyst was the most efficient and durable as compared to titania alone and carbon supported platinum catalysts. Similarly, alumina supported nanocomposite platinum catalyst was more efficient and stable than alumina alone and carbon supported catalysts. Titania is slightly better than the alumina supported catalysts. From the above discussion, it can be concluded that the inclusion of ceramic in support improved efficiency, catalytic activity and durability of Pt/Ceramic-C nanocomposite and can help in the commercialization of polymer electrolyte membrane fuel cells.

REFERENCES

- Ahmed, R., et al., 2014. Synthesis and characterization of ternary Pt-Ni-M/C (M=Cu, Fe, Ce, Mo, W) nano-catalysts for low temperature fuel cells. IOP Conf. Series: Materials Science and Engineering, 60,012044, pp.1-8.
- Ahmed, R., Yamin, T., Ansari, M.S., Chaudhry, M.M., 2009. Effect of Nickel coating on carbon for adsorption of cadmium from aqueous solutions. Can. J. Chem. Eng. 87,pp.448-455
- Ali, S., et.al., 2015. Co@Pt core–shell nanoparticles supported on carbon nanotubes as promising catalyst for methanol electro-oxidation , J. Ind. Eng. Chem., 28 pp. 344–350.
- Antolini, E., Gonzalez, E. R., 2009. Ceramic materials as supports for low-temperature fuel cell catalysts. Solid State Ionics, 180, pp.746-763.
- Armstrong, K. J., 2012. Nanoscale titania ceramic composite supports for PEM fuel cells, J. Mater. Res., 27, pp. 2046-2044.
- Bard, A. J., Faulkner, L.R., 2001. Electrochemical Methods, Fundamentals and applications, J. Wiley & Sons, New York, pp.91-92.
- Borup, R.L., et al., 2006. PEM fuel cell electrocatalyst durability measurements, J. Power Sources, 163, pp.76-81.
- Casolari, B.L., et al., 2014, Model study of a fuel cell range extender for a neighborhood electric vehicle, Int. J. of Hydrogen Energy, 39, pp.10757 – 10787.
- Chalk, S. G., Miller, J. E., 2006. Key challenges and recent progress in batteries, fuel cells, and hydrogen storage for clean energy systems. J. Power Sources 159 , 73-80.
- Chen, C. S., Pan, F. M., 2009. Electrocatalytic activity of Pt nanoparticles deposited on porous TiO_2 supports toward methanol oxidation, J. Applied Catalysis B: Environmental 91, pp. 663-669.
- Costamagana, P., Srinivasan, S., 2001. Quantum jumps in the PEMFC science and technology from the 1960s to the year 2000: Part I. Fundamental scientific aspects, J. Power Sources, 102, pp. 242-252.
- Cullity, B.D., 1956. Elements of x-ray diffraction by, Addison-Wesley, Publishing Company, Inc. Reading, Massachusetts, pp.54-55.
- DOE, 2013. DOE/EIA-0383(2013). Annual Energy Outlook 2013 with Projections to 2040, pp.1-244.
- Duic, N., et al., 2013. Sustainable development of energy, water and environment systems, Applied Energy, 101, pp. 3–5.
- Mueller, S. C., Sandner, P. G., Welpe, I. M., 2015. Monitoring innovation in electrochemical energy storage technologies: A patent-based approach, Applied Energy, 137, pp. 537–544.
- Panwa, N.L., Kaushi, S.C., Kothari, S,. 2011. Role of renewable energy sources in environmental

protection: A review, Renewable and Sustainable Energy Reviews, 15, pp.1513–1524.

- Rajalakshmi, N., Lakshmi, N., Dhathathreyan, K. S., 2008. Nano titanium oxide catalyst support for proton exchange membrane fuel cells. Int. J. Hydrogen Energy 33, pp.7521-7526.
- Ren, X., et al., 2000. Recent advances in direct methanol fuel cells at Los Alamos National Laboratory, J. Power Sources, 86, pp.111–116.
- Romero-Pascual, E., Soler, J., 2014. Modelling of an HTPEM-based micro-combined heat and power fuel cell system with methanol, Int. J. Hydrogen Energy, 39, pp. 4053 – 4059.
- Shao, A. F., et.al., 2010. Evaluation of the performance of carbon supported Pt-Ru-Ni-P as anode catalyst for methanol electrooxidation, Fuel Cells, 10, 472-477.
- Shao, Y., Liu, J., Wang, Y., Lin, Y., 2009. Novel catalyst support materials or PEM fuel cells: Current status and future prospects. J. Mater. Chem. 19, pp.46-59.
- Speder, J., et al., 2014. Comparative degradation study of carbon supported proton exchange membrane fuel cell electrocatalysts. The influence of the platinum to carbon ratio on the degradation rate, J. of Power Sources, 261, pp. 14 – 22.
- Wang, C., Nehrir, M. H., 2008. Power Management of a Stand-Alone Wind/ Photovoltaic/Fuel Cell Energy System. IEEE Transactions on Energy Conversion, 23, pp. 957-967.